Journal of Biomolecular NMR, 9 (1997) 423–436

J-Bio NMR 438

Application of homonuclear 3D NMR experiments and 1D analogs to study the conformation of sialyl Lewis^x bound to E-selectin

Karoline Scheffler[a], Jean-Robert Brisson[b], Rüdiger Weisemann[c], John L. Magnani[d], Wei Tong Wong[d], Beat Ernst[e] and Thomas Peters[a,*]

[a]*Institute for Chemistry, Medical University of Lübeck, Ratzeburger Allee 160, D-23538 Lübeck, Germany*
[b]*Institute for Biological Sciences, National Research Council, Ottawa, ON, Canada K1A 0R6*
[c]*Bruker Analytik GmbH, Silberstreifen, D-76287 Rheinstetten, Germany*
[d]*Glyco Tech Corporation, 14915 Broschart Road, Rockville, MD 20850, U.S.A.*
[e]*Zentrale Forschungslaboratorien, Rosental, Ciba-Geigy AG, CH-4002 Basel, Switzerland*

Received 16 December 1996
Accepted 21 February 1997

Keywords: 3D TOCSY-trNOESY; 1D TOCSY-trNOESY; 1D trNOESY-TOCSY; trNOE; trROE; E-selectin; sialyl Lewis^x

Summary

The conformation of the sialyl Lewis^x tetrasaccharide bound to E-selectin was previously determined from transfer NOE (trNOE) experiments in conjunction with a distance-geometry analysis. However, the orientation of the tetrasaccharide ligand in the binding site of E-selectin is still unknown. It can be predicted that the accurate quantitative analysis of all trNOEs, including those originating from spin diffusion, is one key to analyze the orientation of sialyl Lewis^x in the binding pocket of E-selectin. Therefore, we applied homonuclear 3D NMR experiments and 1D analogs to obtain trNOEs that could not unambiguously be assigned from previous 2D trNOESY spectra, due to severe resonance-signal overlap. A 3D TOCSY-trNOESY experiment, a 1D TOCSY-trNOESY experiment, and a 1D trNOESY-TOCSY experiment of the sialyl Lewis^x/E-selectin complex furnished new interglycosidic trNOEs and provided additional information for the interpretation of trNOEs that have been described before. A 2D trROESY spectrum of the sialyl Lewis^x/E-selectin complex allowed one to identify the amount of spin-diffusion contributions to trNOEs. Finally, an unambiguous assignment of all trNOEs, and an analysis of spin-diffusion pathways, was obtained, creating a basis for a quantitative analysis of trNOEs in the sialyl Lewis^x/E-selectin complex.

Introduction

The orderly extravasation of leukocytes to inflammatory sites is a highly regulated process that involves a diversity of adhesion and signaling molecules. The first step in the recruitment process is the transient 'rolling' interaction of leukocytes along the endothelial cells that line the blood vessels. This phenomenon is based on relatively low-affinity interactions between carbohydrate ligands apparent on leukocyte surfaces and a family of adhesion molecules, called the selectins (Rosen and Bertozzi, 1994; Lasky, 1995; Springer, 1995; Tedder et al., 1995). The selectin family consists of three members: E-, L-, and P-selectin. P- and E-selectin are expressed on the endothelial cell surface in response to inflammatory signals, while L-selectin is constitutively expressed on all classes of circulating leukocytes, and interacts with cognate ligands on endothelial cells. Selectins have an N-terminal carbohydrate-recognition domain (CRD), also called lectin domain. The CRD enables the selectins to recognize carbohydrate ligands on other cells.

The broad participation of selectins in inflammatory diseases has caused great interest in the nature of their carbohydrate ligands as leads for the development of anti-inflammatory agents. All three selectins share a common recognition motif, the sialyl Lewis^x α-D-NeuNAc-(2→3)-β-D-Gal-(1→4)[α-L-Fuc-(1→3)]-β-D-GlcNAc and the related sialyl Lewis^a α-D-NeuNAc-(2→3)-β-D-

*To whom correspondence should be addressed.
Dedicated to Prof. Dr. Hans Paulsen on the occasion of his 75th birthday.

Gal-(1→3)[α-L-Fuc-(1→4)]-β-D-GlcNAc tetrasaccharides (Feizi, 1993; Varki, 1994). A knowledge of the conformational properties of these carbohydrate ligands in solution, and bound to a selectin, is the basis for understanding the molecular features of the selectin–carbohydrate recognition process. A crystal structure for the E-selectin binding domain has been published (Graves et al., 1994), and the bioactive conformation of sialyl Lewis^x bound to E-selectin has been obtained from trNOE experiments in combination with distance-geometry calculations (Scheffler et al., 1995). Several groups have studied the conformational features of sialyl Lewis^x and partial structures thereof in aqueous solution (Wormald et al., 1991; Homans and Forster, 1992; Ichikawa et al., 1992; Lin et al., 1992; Miller et al., 1992). Sialyl Lewis^x in aqueous solution is a complex mixture of conformers, mainly arising from different orientations about the α-D-NeuNAc-(2→3)-β-D-Gal glycosidic linkage, and it has been shown that only one of these conformations is bound by E-selectin (Cooke et al., 1994; Scheffler et al., 1995).

Nevertheless, the orientation of sialyl Lewis^x in the binding site of E-selectin is not known. Analysis of trNOEs using a full relaxation matrix approach that includes chemical exchange, dipolar interactions with protons in the binding site of E-selectin, and conformational changes of the ligand upon binding (Ni and Zhu, 1994; Moseley et al., 1995) could allow one to solve this question. Such a complete analysis requires the unequivocal assignment of all trNOEs, including those originating from spin diffusion. Here, we describe the use of homonuclear 3D NMR experiments and 1D analogs to assign trNOEs and spin-diffusion effects that were ambiguous in previous 2D trNOESY experiments.

Materials and Methods

Preparation of the NMR sample

The IgG-chimera of E-selectin (MW 220 kDa) was prepared as described previously (Scheffler et al., 1995). Sialyl Lewis^x tetrasaccharide (MW 1012 Da) was of synthetic origin (Ernst et al., unpublished results). D_2O (99.998%, Aldrich) was used as solvent, with acetone as a reference (2.22 ppm). The sample volume was 500 µl, containing 6 mg (27 nmol) of E-selectin and 0.81 mg (0.81 µmol) of sialyl Lewis^x tetrasaccharide leading to a 1.62 mM concentration of sialyl Lewis^x and a 54 µM concentration of E-selectin (IgG-chimera). As each IgG/E-selectin chimera has two binding sites, located at the F_{ab} fragments, the total concentration of E-selectin binding sites was 108 µM, resulting in a molar ratio of 1:15 for E-selectin binding sites versus tetrasaccharide ligand. [d_4]Imidazole (Sigma, 30 mM) was used as buffer. In addition, the solution contained NaCl (59 mM) and $CaCl_2$ (1 mM). The pH was 7.4.

Definition of dihedral angles

The dihedral angles about glycosidic linkages were defined as follows: ϕ = H1-C1-O1-Cx (for NeuNAc: C1-C2-O2-Cx), ψ = C1-O1-Cx-Hx (for NeuNAc: C2-O2-Cx-Hx), and ω = O5-C5-C6-O6 (for NeuNAc, corresponding designations were used to indicate the orientation of the side chain), with x being the aglyconic linkage position.

NMR experiments

NMR experiments were carried out on Bruker AMX600 (Institute of Biological Sciences, NRC, Ottawa, Canada), DMX600 (Institute of Biophysical Chemistry, University of Frankfurt, Frankfurt, Germany), and DRX500 (Bruker, Rheinstetten, Germany, and Institute of Chemistry, Medical University of Lübeck, Lübeck, Germany) spectrometers, operating at ^{1}H resonance frequencies of 600.14 MHz (AMX600, DMX600) and 500.13 MHz (DRX500). The sample was not spun. Spectra were recorded at temperatures of 283, 303, and 310 K. Data acquisition and processing was performed with XWINNMR software (Bruker) running on Silicon Graphics Indy workstations. The analysis of 3D NMR spectra was accomplished with the program AURELIA (Bruker). For the 3D TOCSY-trNOESY experiment of the sialyl Lewis^x/E-selectin complex, the 3D TOCSY-NOESY pulse sequence was used (Griesinger et al., 1989; Oschkinat et al., 1990). The 3D spectrum was acquired in phase-sensitive mode using time-proportional phase incrementation (Marion and Wüthrich, 1983) on a DRX500 spectrometer (Bruker). The temperature was 310 K, and the spectral width was set at 3000 Hz (6 ppm) for t_1, t_2, and t_3. Presaturation of the HDO signal during the relaxation delay was achieved using a selective 180° pulse. The relaxation delay was set at 1.2 s, and the acquisition time was 0.341 s, resulting in a total relaxation delay of 1.541 s. For the TOCSY transfer, a spin-lock field of a duration of 52 ms and a strength of 6.25 kHz was generated with an MLEV-17 sequence (Bax and Davis, 1985; Subramanian and Bax, 1987). 1K real data points were acquired during t_3, with 256 increments in t_2 and 128 increments in t_1. At the beginning of the 3D experiment 32 dummy scans were performed and eight transients were acquired for each data point $S(t_1,t_2,t_3)$, where S stands for signal. The total acquisition time was approximately 4 days. Prior to Fourier transformation, the data matrices were zero-filled to give a final matrix of a size of 1K (t_3) × 512 (t_2) × 256 (t_1) and squared cosine bell functions were applied as window functions in each dimension. The resulting digital resolution was 3 Hz per data point for ω_3, 5.9 Hz per data point for ω_2, and 11.7 Hz per data point for ω_1. Selective NMR experiments and 1D analogs of 3D NMR experiments were recorded on the DRX500 spectrometer located at the Institute of Chemistry, Medical University of Lübeck. 1D trNOESY experiments were performed using the 1D NOESY pulse

sequence according to the literature (Kessler et al., 1986, 1991), with 32K data points and 1K to 8K scans each. A spectral width of 10 000 Hz (20 ppm) was chosen. Relaxation delays were between 1 and 2 s, resulting in total experiment times between 1 and 12 h, depending on the number of scans and the mixing time. Selective excitation was achieved with self-refocussing 270° Gaussian pulses (Emsley and Bodenhausen, 1989). Presaturation of the HDO signal was not necessary. 1D trNOESY-TOCSY and 1D TOCSY-trNOESY experiments were performed using the published pulse sequences for 1D NOESY-TOCSY and 1D TOCSY-NOESY (Uhrín et al., 1993, 1994). Presaturation of the HDO signal was accomplished by a low-power pulse at the HDO resonance frequency during the relaxation delay. The relaxation delay was set at 1.5 s, and together with the acquisition time of 1.64 s a total relaxation delay of 3.14 s resulted. Four dummy scans were recorded at the beginning of each experiment, and 8K scans were recorded for each spectrum. The free induction decay consisted of 16K data points. The total experiment time was between 7 and 12 h, depending on the length of the mixing time. Selective excitation was achieved utilizing self-refocussing 270° Gaussian pulses (Emsley and Bodenhausen, 1989). The TOCSY transfer was achieved with the MLEV-17 pulse sequence. The attenuation of the 90° and 180° pulses of MLEV-17 was adjusted to give a strength of the spin-lock field of ca. 10 kHz. The duration of the spin-lock field was then optimized using 1D TOCSY experiments (Kessler et al., 1991), which allowed experimental determination of the maximum magnetization transfer to the desired proton.

Phase-sensitive 2D trNOESY experiments were recorded on the AMX600 and DMX600 spectrometers located in Ottawa, Canada and Frankfurt, Germany, respectively. A standard 2D NOESY pulse sequence was used. The relaxation time was set at 1.5 s. The acquisition time was 0.34 s to give a total relaxation delay of 1.84 s. To suppress ^{1}H resonances of E-selectin, a spin-lock pulse with a strength of ca. 5 kHz and a duration of 10 ms was applied after the 90° excitation pulse (Scherf and Anglister, 1993). Presaturation of the HDO resonance was achieved by low-power irradiation during the relaxation delay and during the mixing time. The spectral widths were set at 3000 Hz (5 ppm) or 6666 Hz (11.11 ppm). A total of 512 increments were recorded in t_1 with 32 transients and 2K data points each. At the beginning of the 2D experiment 32 dummy scans were performed . Zero-filling and multiplication of the time domain data with squared cosine functions in both dimensions, t_1 and t_2, resulted in a $2K \times 1K$ data matrix. 2D Fourier transformation gave the final 2D spectra. For spectra that were acquired on the AMX600 spectrometer, a third-order polynomial baseline correction was applied in both dimensions, F1 and F2. For spectra from the DMX and the DRX spectrometers where digital data acquisition was implemented, a baseline correction was not necessary. 2D trROESY experiments were recorded using a standard 2D ROESY pulse sequence with the same number of data points in t_1 and t_2 as described for the 2D NOESY experiments. During the mixing time a single spin-lock pulse was applied, with a strength of 5 kHz and a duration of 150 ms. The relaxation delay was 1.5 s. The acquisition time was 0.15 s to give a total relaxation delay of 1.65 s. The spectral width was 6666 Hz (11.11 ppm). The carrier frequency of the spin-lock pulse was located away from relevant ^{1}H resonance frequencies, at 6.6 ppm, to suppress TOCSY magnetization transfer (Bax, 1988). The total experiment time of the 2D trNOESY and 2D trROESY experiments was around 10 h each, depending on the duration of the mixing time.

MMC simulations

MMC simulations (Peters et al., 1993) for sialyl Lewis^x with the program GEGOP (Stuike-Prill and Meyer, 1990) were performed as described previously (Scheffler et al., 1995). A set of conformations was generated with the temperature parameter set at 2000 K and with 1×10^6 macrosteps. The maximum step size was 20° (ϕ,ψ) and 25° (ω), giving an overall acceptance ratio of 46%. The high-temperature parameter was chosen to ensure that all sterically possible conformations were considered. The distance constraints that were used previously (see Table 2 in Scheffler et al. (1995)), except for the distance constraint between the protons H5^F and H6^G, were applied to the set of conformations generated, using a MATLAB routine. All calculations were performed on a Silicon Graphics Indy II workstation.

Results and Discussion

The present study is an extension of our previous NMR analysis of the bioactive conformation of sialyl Lewis^x (Scheffler et al., 1995). For an understanding, it is necessary to summarize the earlier results. In Fig. 1a, the structure of the sialyl Lewis^x tetrasaccharide is shown with the labeling of the individual pyranose rings as they are referred to in the text. Figure 1b comprises interglycosidic trNOEs that were essential for the deduction of the conformation of sialyl Lewis^x bound to E-selectin, and Fig. 1c is a stereo representation of the bioactive conformation of sialyl Lewis^x. The bioactive conformation of sialyl Lewis^x was established utilizing trNOE data from 2D trNOESY experiments in conjunction with a distance-geometry analysis that was based on the isolated spin-pair approximation and on high-temperature Metropolis Monte Carlo simulations (Scheffler et al., 1995). ^{1}H NMR chemical shifts are listed in Table 1, and dihedral angles for the individual glycosidic linkages in the bound state are given in the legend to Fig. 1c. As we aim at a quantitative analysis of trNOE data in order to finally infer the

a

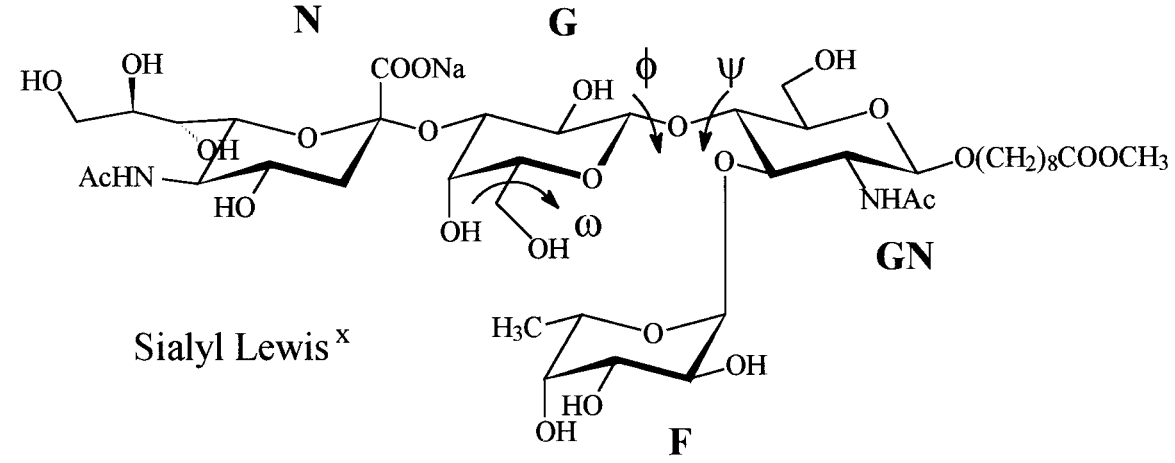

b

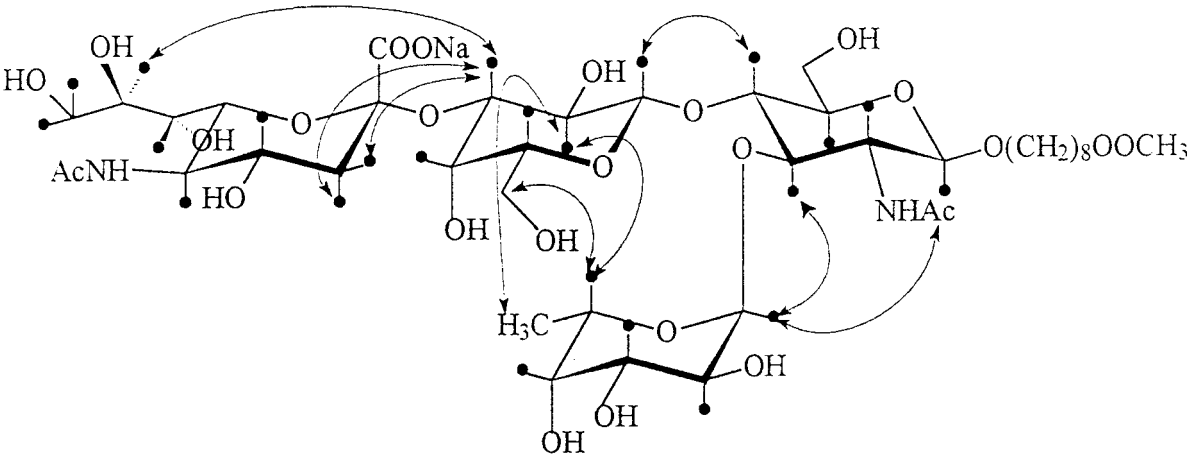

c

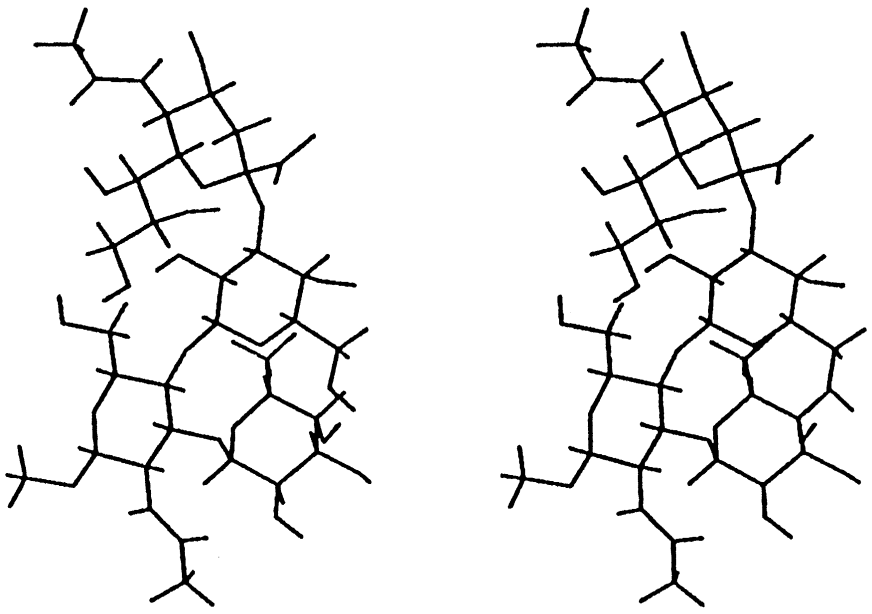

Fig. 1. (a) Structural formula of the synthetic sialyl Lewis^x tetrasaccharide used in this study. (b) Interglycosidic trNOEs that have been used as distance constraints in a previous study (Scheffler et al., 1995). The arrows between $H3^G$ and the protons $H3^N_{ax,eq}$ symbolize 'negative' constraints because no trNOEs are observed for sialyl Lewis^x bound to E-selectin. (c) Conformation of sialyl Lewis^x bound to E-selectin. The dihedral angles at the glycosidic bonds are: $\phi_{N\text{-}G} = -76° +/- 10°$, $\psi_{N\text{-}G} = 6° +/- 10°$, $\phi_{G\text{-}GN} = 39° +/- 10°$, $\psi_{G\text{-}GN} = 12° +/- 6°$, $\phi_{F\text{-}GN} = 38° +/- 7°$, $\psi_{F\text{-}GN} = 26° +/- 6°$ (values were taken from Scheffler et al. (1995)).

TABLE 1
^{1}H NMR CHEMICAL SHIFTS FOR THE TETRASACCHARIDE SIALYL LEWIS^x IN D_2O AT 303 K AND 600 MHz

	NeuNAc	Gal	GlcNAc	Fuc	Spacer -O$(CH_2)_8$-COOMe
H1		4.51	4.51	5.09	
H2		3.52	3.89	3.68	
H3		4.08	3.85	3.88	
$H3_{ax}$	1.79				
$H3_{eq}$	2.76				
H4	3.68	3.92	3.92	3.77	
H5	3.86	3.58	3.58	4.81	
H6	3.66				
$H6_{pro\,R}$		3.68	3.88		
$H6_{pro\,S}$		3.68	4.00		
CH_3-6				1.16	
H7	3.59				
H8	3.89				
$H9_{pro\,R}$	3.64				
$H9_{pro\,S}$	3.87				
N-CH_3	2.03		2.01		
$4\times CH_2$					1.28
CH_2					1.52
CH_2					1.59
CH_2					2.38
-O-$CH_{pro\,R}$-					3.58[a]
-O-$CH_{pro\,S}$-					3.87[a]
-$COOCH_3$					3.68

Reference signal: δ(acetone) = 2.22. Some typographic mistakes that were found in our previous table (Scheffler et al., 1995) are corrected here.
[a] These values can be interchanged.

orientation of sialyl Lewis^x in the binding site of E-selectin, an unequivocal assignment of all trNOEs that includes the analysis of spin-diffusion contributions to trNOEs and the analysis of possible spin-diffusion pathways is required. In the following, we will discuss trNOEs and spin-diffusion effects that are substantial for a complete conformational analysis but that have not been unambiguously assigned yet.

The interglycosidic trNOE $H3^G$/$H8^N$

The observation of an interglycosidic trNOE $H3^G$/$H8^N$ (Fig. 3c) was essential for the experimental determination of the bioactive conformation of the sialyl Lewis^x tetrasaccharide (Scheffler et al., 1995). The assignment of this trNOE was based on proton chemical shift data and on steric factors. In particular, it was found that the proton $H2^{GN}$ resonates at the same frequency as $H8^N$ (3.89 ppm), and the chemical shift values for the protons $H3^F$ and $H6^{GN}_{pro\,S}$ differ only by 0.01 ppm from this value (Table 1). For steric reasons, it was ruled out that either of the protons $H2^{GN}$, $H6^{GN}_{pro\,S}$, or $H3^F$ is a direct dipolar coupling partner for $H3^G$, which left $H8^N$ as the only reasonable alternative. However, this is not an experimental proof.

To achieve this, a 3D TOCSY-trNOESY experiment that employs the 3D TOCSY-NOESY pulse sequence was performed. The 3D TOCSY-NOESY experiment has been a valuable tool for the analysis of the solution structure of proteins, especially when $^{13}C/^{15}N$ isotopic enrichment was not available (Griesinger et al., 1989; Oschkinat et al., 1990). Recently, the experiment was also applied in the course of the conformational analysis of a glycoprotein at natural $^{13}C/^{15}N$ abundance (De Beer et al., 1996). Alternatively, a 3D NOESY-TOCSY experiment could have been performed (Vuister et al., 1989). The TOCSY step in the 3D TOCSY-trNOESY experiment represents a 'built-in spin-lock filter' (Scherf and Anglister, 1993) that suppresses unwanted transversal magnetization originating from protein protons. Consequently, the 3D TOCSY-trNOESY spectrum of the sialyl Lewis^x/E-selectin complex was not contaminated with protein proton-background signals. An ω_1/ω_2-2D plane extracted from the 3D TOCSY-trNOESY spectrum at the resonance frequency $\omega_3 = \delta(H3^G)$ is shown in Fig. 2. The 2D plane contains trNOEs originating from $H3^G$ on the diagonal, marked as NOESY line in Fig. 2. The trNOE between $H3^G$ and $H8^N$ is indicated on this line. Because of limited digital resolution, the peak appears as a shoulder only. However, the most important feature in this 2D plane is the occurrence of an off-diagonal peak, labeled c in Fig. 2. This peak arises from the following magnetization transfer: $H7^N/H9^N_{pro\,R}$-*TOCSY*→$H8^N$-*trNOESY*→$H3^G$, linking $H3^G$ not only to its direct coupling partner but also to protons that are spin–spin coupled to the dipolar coupling partner. Therefore, the corresponding trNOE observed in the 2D trNOESY spectra can only arise from a dipolar interaction between $H3^G$ and $H8^N$. In this regard, it is important to mention that for free sialyl Lewis^x a significant cross peak between $H3^G$ and $H8^N$ is not observed at 310 K but only at lower temperatures, e.g. at 283 K (data not shown). This has already been observed by other authors (Breg et al., 1989; Rutherford et al., 1994), and is due to the tetrasaccharide's tumbling time τ_c that places $\omega\tau_c$ close to one. It follows that at 310 K a trNOE between $H3^G$ and $H8^N$, detected for the sialyl Lewis^x/E-selectin complex, has no or only a negligible contribution from the corresponding NOE of free sialyl Lewis^x tetrasaccharide.

Although not attempted here, a quantitative interpretation of NOEs from homonuclear 3D TOCSY-NOESY spectra is possible because NOE cross peaks on the same line all lack the same amount of signal intensity due to the TOCSY transfer. Qualitatively, it is seen that the trNOE between $H5^G$ and $H3^G$ (cross peak a) is more intense than that between $H6^G$ and $H3^G$ (cross peak b). This is explained from the ring geometry of the β-D-Gal-pyranose ring, where H3 and H5 have a trans-diaxial orientation and thus a short internuclear distance, whereas the distance between H3 and H6 is ca. 4 Å, depending on the orientation of the hydroxy-methyl group. Cross peak b is probably due to spin diffusion via $H5^G$. As the

digital resolution of a homonuclear 3D experiment is limited, critical assignments have to be performed with care. One solution is to acquire a selective 2D TOCSY-NOESY spectrum (de Waard et al., 1992). Here, we performed a 1D trNOESY-TOCSY experiment to unambiguously prove the assignment of the $H3^G/H8^N$ trNOE (Fig. 3). A 1D trNOESY experiment with selective excitation of $H3^G$ is shown in Fig. 3a, and the trNOE between $H3^G$ and $H8^N$ is indicated. Figure 3b shows the corresponding 1D trNOESY-TOCSY experiment, where the selective excitation of $H3^G$ for the trNOESY step was followed by selective excitation at the resonance frequency of $H8^N$ for the subsequent TOCSY step. This experiment unequivocally unravels the spin-coupling partners of the proton that is the dipolar coupling partner of $H3^G$. It is obvious that the spin–spin coupling partners detected by the TOCSY step are the side-chain protons $H7^N$, $H9^N_{proR}$, and $H9^N_{proS}$ of neuraminic acid (Fig. 3b). Magnetization transfer from $H8^N$ to the pyranose-ring protons of neuraminic acid cannot occur during the TOCSY step, because the vicinal coupling constant between $H7^N$ and $H6^N$ (1.8 Hz (Breg et al., 1989)) is too small for an efficient TOCSY transfer. To summarize, the NMR experimental data presented here unequivocally confirm the original assignment of the $H3^G/H8^N$ trNOE.

Analysis of trNOEs at the β-(1→4)-glycosidic linkage between Gal and GlcNAc

The chemical shifts of the anomeric protons of the β-D-GlcNAc residue and the β-D-Gal residue are identical (Table 1). Therefore, our previous analysis of the conformation of the β-(1→4)-glycosidic linkage of sialyl Lewis^x bound to E-selectin had to be based only on an estimation of the interglycosidic trNOE between $H1^G$ and $H4^{GN}$. Moreover, other interglycosidic trNOEs at this linkage could not be identified unequivocally. An ω_1/ω_3-2D plane

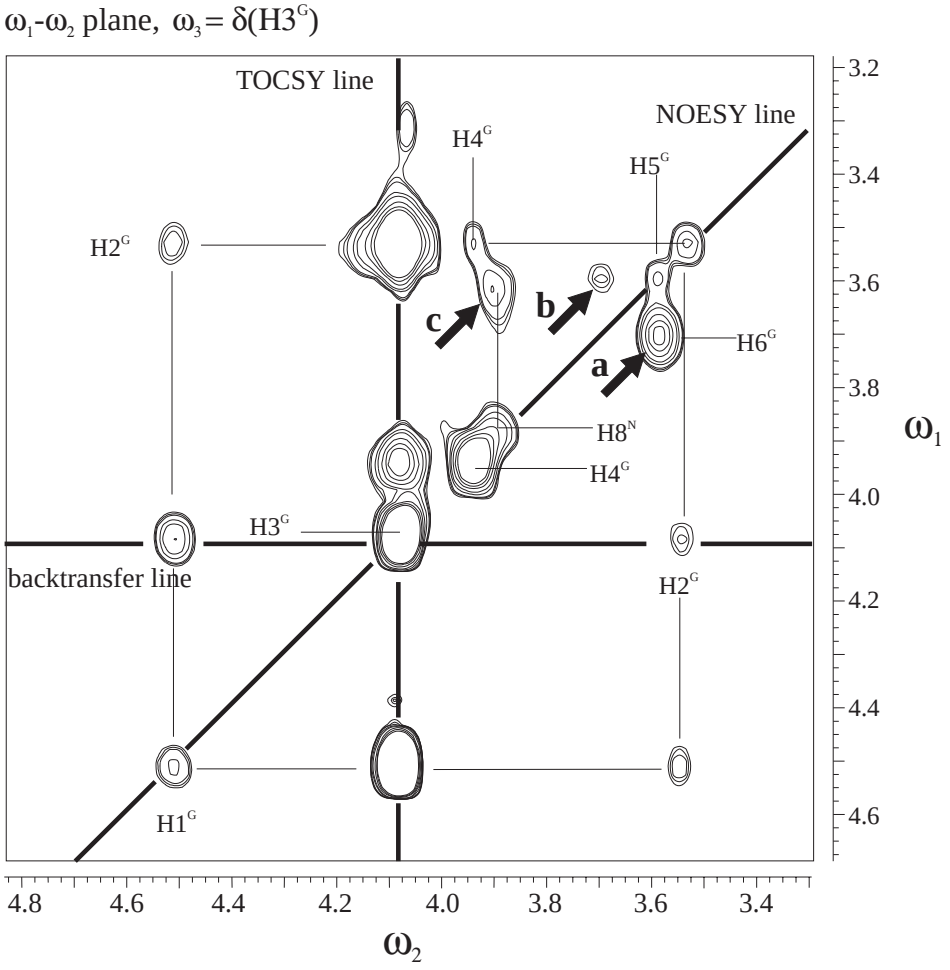

Fig. 2. ω_1/ω_2 slice of the 3D TOCSY-trNOESY spectrum (500 MHz, 310 K) at $\omega_3 = \delta(H3^G)$. All cross peaks are due to individual magnetization-transfer pathways that consist of a TOCSY step during t_1 (*-TOCSY→*) and a trNOESY step during t_2 (*-trNOESY→*). In general, a cross peak with the coordinates $\omega_1 = \delta(A)$ and $\omega_2 = \delta(B)$ originates from a magnetization transfer A *-TOCSY→* B *-trNOESY→* $H3^G$. Therefore, cross peaks a, b, and c are due to magnetization transfers $H6^G$ *-TOCSY→* $H5^G$ *-trNOESY→* $H3^G$, $H5^G$ *-TOCSY→* $H6^G$ *-trNOESY→* $H3^G$, and ($H7^N$,$H9^N$) *-TOCSY→* $H8^N$ *-trNOESY→* $H3^G$. For a comprehensive description of the interpretation of 3D TOCSY-NOESY spectra, see Oschkinat et al. (1990,1994).

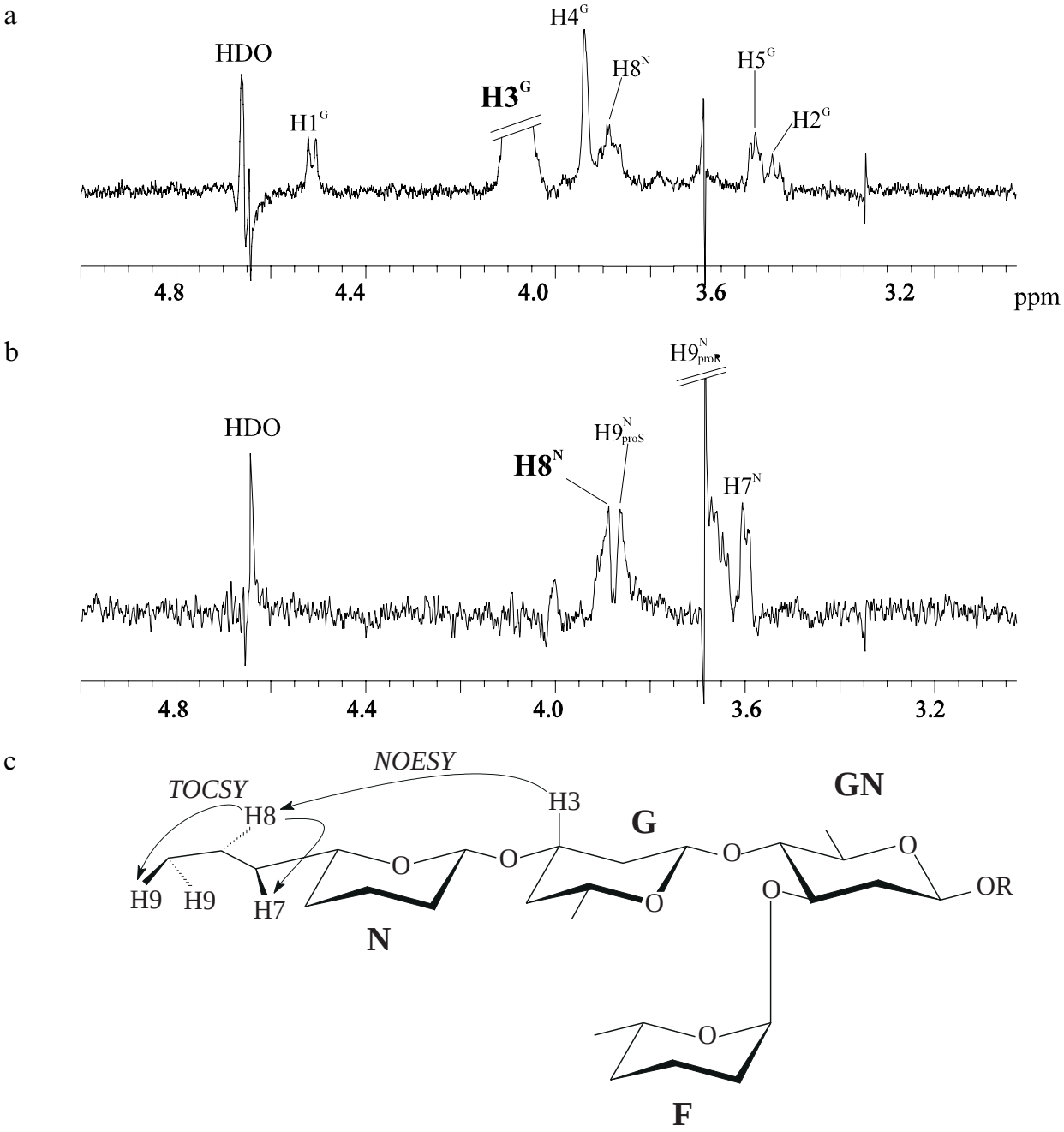

Fig. 3. (a) 1D-trNOESY spectrum of sialyl Lewis^x bound to E-selectin at 500 MHz and 310 K. The mixing time was 200 ms. Selective excitation of $H3^G$ furnished an interglycosidic trNOE to $H8^N$. (b) 1D trNOESY-TOCSY of sialyl Lewis^x bound to E-selectin at 500 MHz and 310 K. The duration of the spin-lock field was 46.7 ms, and the mixing time was 200 ms. For the trNOESY step, $H3^G$ was selectively excited; for the TOCSY step it was $H8^N$. A magnetization transfer $H3^G$ -*trNOESY*→ $H8^N$ -*TOCSY*→ $H7^N/H9^N_{proR}/H9^N_{proS}$ is observed. The dispersion signal at 3.68 ppm in both spectra, (a) and (b), is due to imperfect cancellation of the ^{1}H resonance signal of the *O*-methyl group of the spacer (see Table 1). (c) Partial structural formula of sialyl Lewis^x showing the magnetization transfer during the 1D trNOESY-TOCSY experiment.

from the 3D TOCSY-trNOESY spectrum at $\omega_2 = \delta(H1^G, H1^{GN})$ (Fig. 4) shows that all trNOEs exclusively originating from $H1^G$ can be detected in trace a, at $\omega_1 = \delta(H3^G)$. The value of the chemical shift of $H3^G$ is different from that of other protons of sialyl Lewis^x (Table 1) and, therefore, all trNOEs in trace a must originate from a magnetization transfer $H3^G$ -*TOCSY*→ $H1^G$ during the first part of the 3D TOCSY-trNOESY experiment, separating them from trNOEs that originate from $H1^{GN}$. In the 3D experiment, the following trNOEs can be observed without spectral overlap (Fig. 4, trace a): $H1^G$ -*trNOESY*→ ($H3^G$,$H6^{GN}_{proS}$,$H4^G$,$H6^{GN}_{proR}$,$H6^G$,$H5^G$,$H2^G$). It should also be noticed that the interglycosidic trNOEs between $H1^G$ and $H6^{GN}_{proS}$,$H6^{GN}_{proR}$ have not been described before. At $\omega_1 =$

$\delta(H2^{G})$, the same pattern of trNOEs is observed (trace c in Fig. 4). The protons $H2^{GN}$, $H3^{GN}$, and $H4^{GN}$ have very similar chemical shift values (Table 1), and constitute a system of higher order. Nevertheless, it is also possible to separately observe the trNOEs originating from $H1^{GN}$ in this 2D plane. They are found in trace b of Fig. 4, at $\omega_1 = \delta(H2^{GN},H3^{GN},H4^{GN})$. These trNOEs are not of much interest for the conformational analysis of the sialyl Lewis^x/E-selectin complex and are not discussed further.

For a quantitative analysis of interglycosidic trNOEs at the β-(1→4)-glycosidic linkage, a 3D spectrum is not ideal because of the poor digital resolution. A 1D TOCSY-trNOESY experiment is more appropriate. Here, selective excitation of $H3^{G}$ for the TOCSY step was followed by selective excitation of $H1^{G}$ for the subsequent trNOESY transfer. A spectrum (Fig. 5) is obtained that contains only the desired trNOEs originating from $H1^{G}$ and that allows precise integration of these trNOEs.

Analysis of 'long-range interactions' and spin-diffusion effects

Several cross peaks that were observed in our previous 2D trNOESY experiments indicated long-range interactions, i.e. interactions between protons that are not expected to be closer to each other than ca. 4 Å. In general, the intensity of such cross peaks is low, and an unambiguous assignment was not possible so far. It can be expected that most of these long-range effects originate from spin diffusion. Therefore, we did not use these effects in our distance-geometry analysis of sialyl Lewis^x bound to E-selectin. For the purpose of a detailed quantitative analysis, these long-range interactions must be assigned, and trNOEs must be distinguished from spin-diffusion effects.

In the 2D trNOESY spectrum of the sialyl Lewis^x/E-selectin complex, a weak cross peak was observed between $H1^{F}$ and either $H1^{G}$ or $H1^{GN}$ (see Fig. 7a). An assignment was impossible because $H1^{G}$ and $H1^{GN}$ have the same

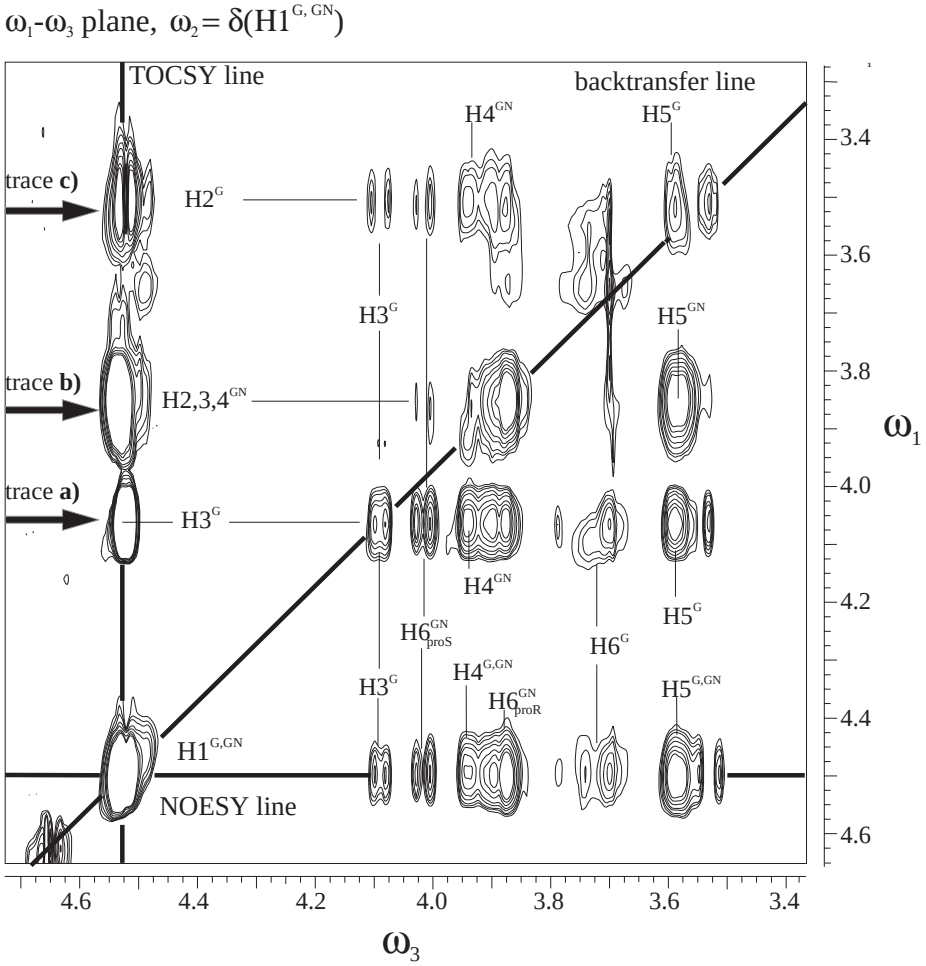

Fig. 4. ω_1/ω_3 slice of the 3D TOCSY-trNOESY spectrum (500 MHz, 310 K) at $\omega_2 = \delta(H1^{GN,G})$. All cross peaks are due to individual magnetization-transfer pathways that consist of a TOCSY step during t_1 (*-TOCSY→*) and a trNOESY step during t_2 (*-trNOESY→*). In general, a cross peak with the coordinates $\omega_1 = \delta(A)$ and $\omega_3 = \delta(B)$ originates from a magnetization transfer A *-TOCSY→* $H1^{G,GN}$ *-trNOESY→* B. The TOCSY transfer allows one to spread trNOEs that originate from $H1^{G}$ or $H1^{GN}$ on other ^1H resonance signals along the ω_1 axis. Therefore, traces a and c contain trNOEs of $H1^{G}$, and trace b shows trNOEs for $H1^{GN}$.

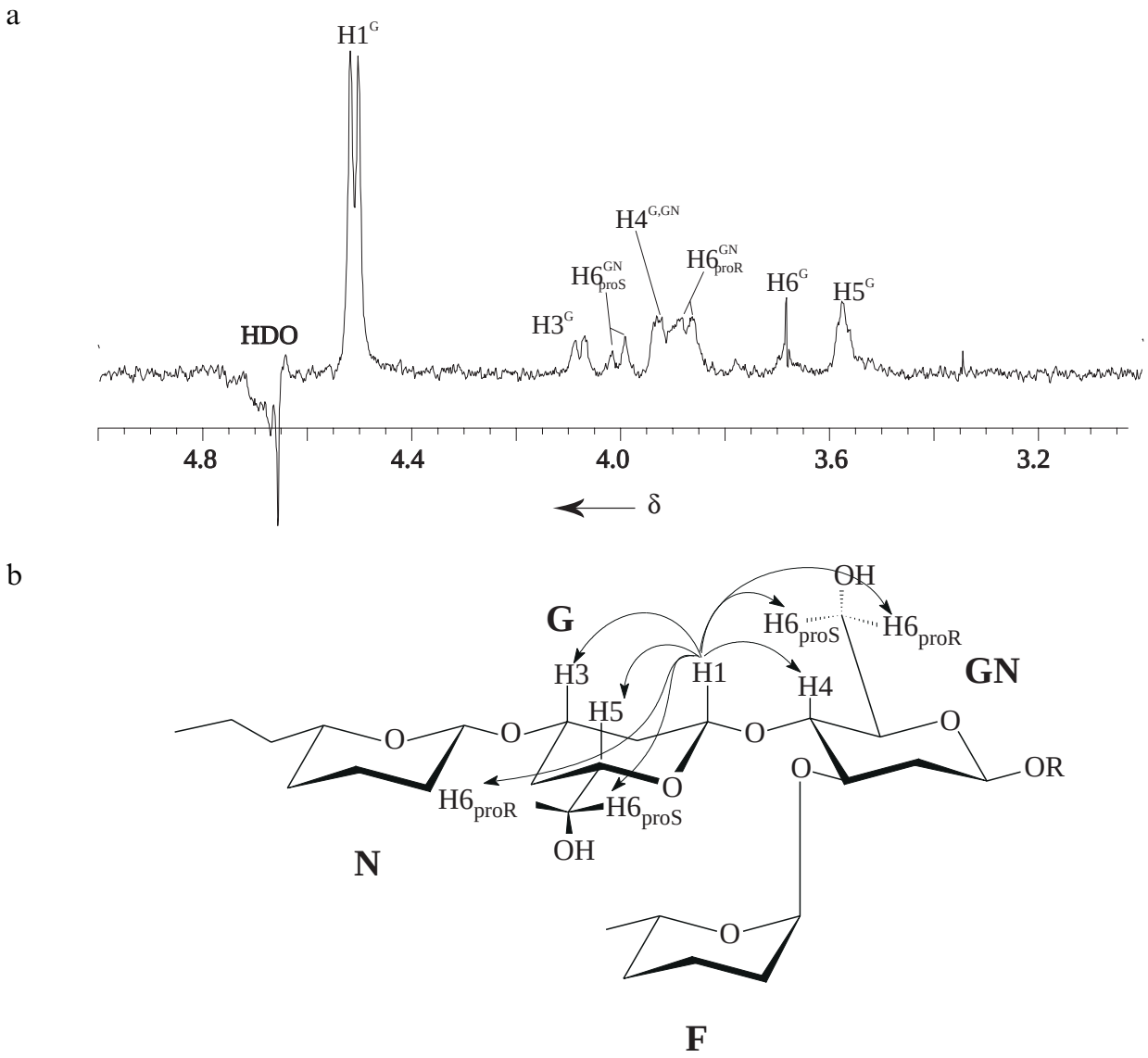

Fig. 5. (a) A 1D TOCSY-trNOESY spectrum is shown (500 MHz, 310 K). The duration of the spin-lock field was 47 ms, and the mixing time was set at 200 ms. For the TOCSY transfer, $H3^G$ was selectively excited. For the subsequent trNOESY transfer, $H1^G$ was selectively excited. Although $H1^G$ and $H1^{GN}$ have the same chemical shift values, only trNOEs from $H1^G$ are observed. The dispersion signal at 3.68 ppm is due to imperfect cancellation of the ^1H resonance signal of the *O*-methyl group of the spacer (cf. Fig. 3 and see Table 1). (b) Partial structural formula of sialyl Lewis^x showing the observed interglycosidic trNOEs.

value of the chemical shift. An ω_1/ω_2-2D plane taken from the 3D TOCSY-trNOESY spectrum at $\omega_3 = \delta(H1^F)$ allows one to identify this 2D trNOESY cross peak (Fig. 6). No cross peaks originating from TOCSY transfer from protons of the β-D-Gal residue are observed and, therefore, the 2D trNOESY cross peak is exclusively due to an interaction between $H1^F$ and $H1^{GN}$. A weak trNOESY cross peak was also observed between $H5^F$ and either $H1^G$ or $H1^{GN}$ which could not be discriminated (Fig. 7a). All cross peaks in an ω_1/ω_2-2D plane at $\omega_3 = \delta(H5^F)$ are due to a trNOESY transfer to $H5^F$ and, therefore, a cross peak at $\omega_1(H1^{GN})/\omega_2(H2^{GN},H3^{GN})$ in this plane demonstrates that a long-range interaction between $H2^{GN}$ and/or $H3^{GN}$ and $H5^F$ exists (data not shown). A corresponding symmetrical cross peak is observed at $\omega_1(H2^{GN},H3^{GN})/\omega_2(H1^{GN})$, showing that there is also a long-range interaction between $H1^{GN}$ and $H5^F$. In the 2D trNOESY spectrum, this interaction cannot be observed, because it interferes with the trNOE between $H3^F$ and $H5^F$.

Two other cross peaks in the 2D trNOESY spectrum were tentatively assigned as trNOEs between $H5^F$ and $H6^G$ and between $H5^F$ and $H5^G$, but both assignments were not unambiguous because $H5^G$ and $H5^{GN}$ have the same resonance frequency, and $H6^G$ cannot be distinguished from $H2^F$ (Table 1). An ω_1/ω_2-2D plane of the 3D TOCSY-trNOESY spectrum at $\omega_3 = \delta(H5^F)$ leads to an unequivocal assignment (data not shown). Cross

peaks observed at positions $\omega_1(H5^G)/\omega_2(H6^G)$ and $\omega_1(H6^G)/\omega_2(H5^G)$ prove the magnetization transfers $H5^G$-*TOCSY*→ $H6^G$ -*trNOESY*→ $H5^F$ and $H6^G$ -*TOCSY*→ $H5^G$ -*trNOESY*→ $H5^F$. At the same time, cross peaks are observed at $\omega_1(H3^{GN})/\omega_2(H5^{GN})$ and $\omega_1(H5^{GN})/\omega_2(H3^{GN})$, demonstrating that long-range interactions also exist between $H3^{GN}$ and $H5^F$, as well as between $H5^{GN}$ and $H5^F$. Consequently, the previous assignment was incomplete.

Several trNOEs that have not been unambiguously assigned yet are originating from the fucose methyl group and the methyl groups of the two *N*-acetyl functions. A comparison of 2D NOESY spectra of free sialyl Lewis^x

a

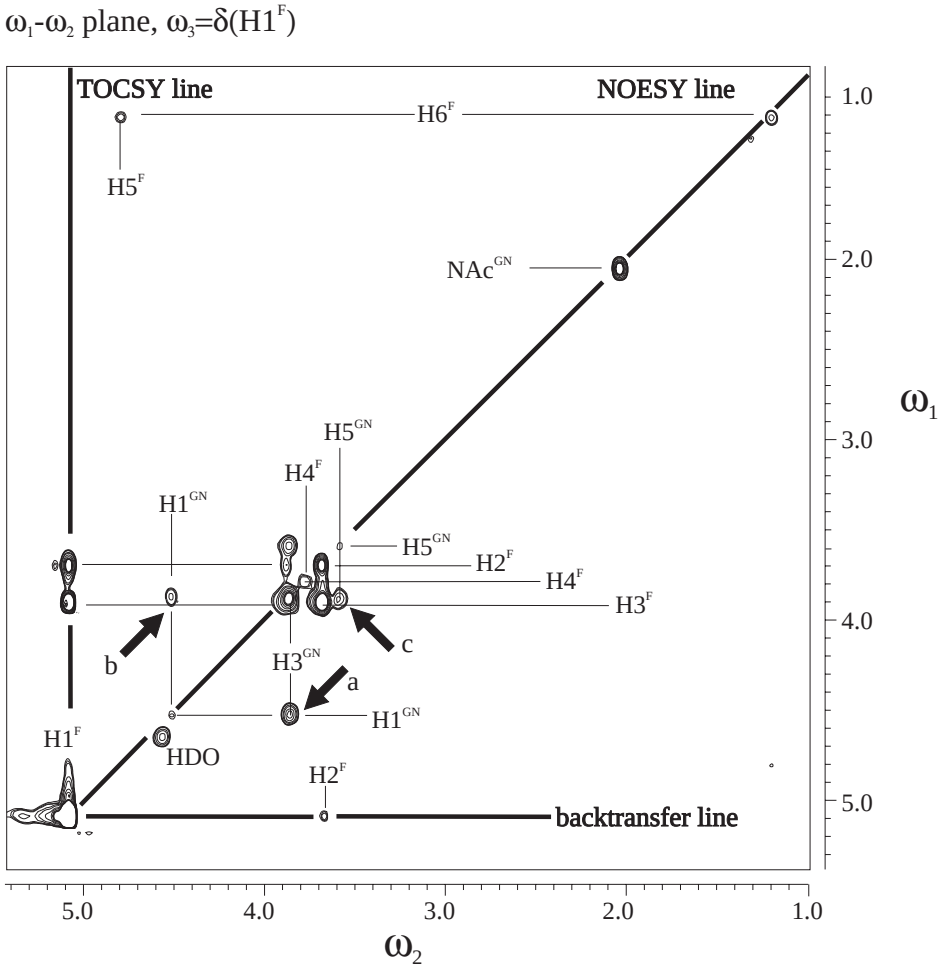

b

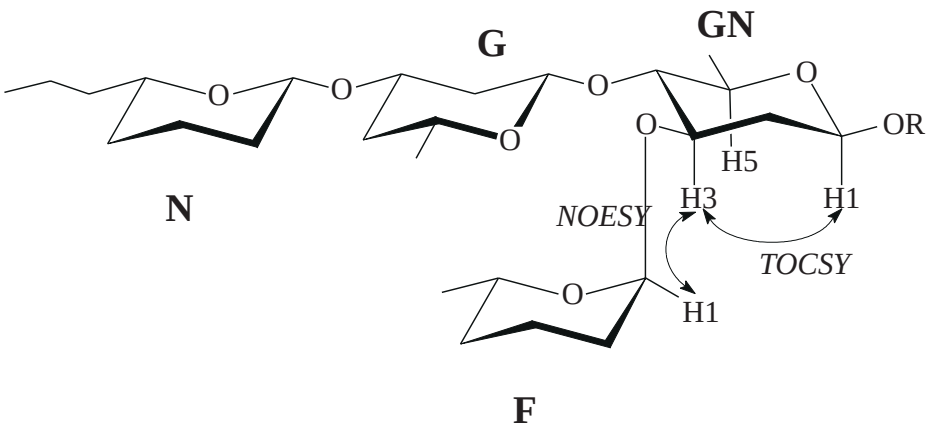

Fig. 6. (a) ω_1/ω_2 slice of the 3D TOCSY-trNOESY spectrum (500 MHz, 310 K) at $\omega_3 = \delta(H1^F)$. See also the legend to Fig. 2 for further explanations. Cross peaks a, b, and c are due to magnetization transfers $H1^{GN}$ -*TOCSY*→ $H3^{GN}$ -*trNOESY*→ $H1^F$, $H3^{GN}$ -*TOCSY*→ $H1^{GN}$ -*trNOESY*→ $H1^F$, and $H3^{GN}$ -*TOCSY*→ $H5^{GN}$ -*trNOESY*→ $H1^F$, respectively. (b) Partial structural formula of sialyl Lewis^x showing the observed interglycosidic trNOEs.

tetrasaccharide with corresponding 2D trNOESY spectra of the sialyl Lewis^x/E-selectin complex reveals notable differences in the cross-peak patterns that connect the protons of the fucose methyl group and the *N*-acetyl methyl groups of *N*-acetyl neuraminic acid and *N*-acetyl glucosamine with ring protons. For free sialyl Lewis^x NOEs involving the *N*-acetyl methyl groups are very weak, but when bound to E-selectin trNOEs of significant size can be observed, as is shown in Fig. 7c. This part of the 2D trNOESY spectrum also contains the cross peaks from the fucose methyl group. From ω_1/ω_2-2D planes at $\omega_3 = \delta(NAc^N)$, $\delta(NAc^{GN})$, and $\delta(CH_3\text{-}6^F)$, an assignment of all cross peaks was accomplished, as indicated in Fig. 7.

Recently, it has been shown that spin-diffusion effects in trNOESY experiments can be identified qualitatively from trROESY experiments (Lian et al., 1994; Arepalli et al., 1995; Asensio et al., 1995; Weimar et al., 1995). Cross peaks arising exclusively from spin diffusion have the same sign as diagonal signals, i.e. they are negative, and thus easy to distinguish from direct trROEs that are positive. A lack of cross peaks in the trROESY spectra is due to either a lack of magnetization transfer or to a cancellation of direct ROEs (positive) that arise from not-bound ligand molecules, and spin-diffusion effects (negative). Also, indirect trROEs can be very small, especially if more than one relay proton is involved (Lian et al., 1994), and several changes of the sign of the trROE occur. In general, if a negative trROE or no trROE is observed where a trNOE was observed, the interaction is most likely due to spin diffusion. Therefore, we applied 2D trROESY experiments to separate 'true' trNOEs from spin-diffusion effects.

First, the observation of a significant trROE between $H3^G$ and $H8^N$ confirms a direct dipolar interaction between the two spins (data not shown). The partial 2D trNOESY spectra in Figs. 7a and c show spectral regions where cross peaks between anomeric protons and pyranose-ring protons occur (Fig. 7a), and where cross peaks between the *N*-acetyl groups and the fucose methyl group $CH_3\text{-}6^F$ and pyranose-ring protons are observed (Fig. 7b). In Figs. 7b and d, the corresponding portions of the 2D trROESY spectrum are shown. It is obvious that some of the cross peaks that are present in Figs. 7a and c are not observed in Figs. 7b and d, and spin diffusion must be assumed. Important observations will be discussed in the following, and a summary is given in Table 2.

In our previous study, the interaction between $H5^F$ and $H6^G$ (peak 6, Fig. 7a) has been interpreted as a direct trNOE, and contributions from spin diffusion were neglected. Therefore, this trNOE was used as a distance constraint. However, a comparison of Figs. 7a and 7c shows that the cross peak between $H5^F$ and $H6^G$ has almost zero intensity in the 2D trROESY spectrum (peak 6) and, therefore, spin-diffusion contributions superimpose the direct trNOE (Figs. 7a and c). The relative amounts of direct and indirect interactions are difficult to determine, but to estimate the importance of the $H5^F/H6^G$ distance constraint we performed a new distance-geometry analysis based on a high-temperature MMC simulation of sialyl Lewis^x without including the $H5^F/H6^G$ distance constraint. A bioactive conformation of sialyl Lewis^x was obtained that is very similar to the one shown in Fig. 1c, and all dihedral angles about the glycosidic linkages are within the experimental limits determined previously (see the legend to Fig. 1c). It follows that the distance constraint $H5^F/H6^G$ is less consequential for a simple distance-geometry analysis. It can be hypothesized that a relay proton attached to E-selectin is involved in the spin-diffusion process observed, but as our attempts to record trNOEs between sialyl Lewis^x protons and E-selectin protons failed, this cannot be proven. It is interesting, however, to note that it was observed already in our previous study (Scheffler et al., 1995) that the trNOE between $H5^F$ and $H2^G$ is much weaker than the corresponding NOE for the not-bound ligand. The protons $H5^F$, $H2^G$, and $H6^G$ are neighbors, and therefore it could be that in both cases the same spin-diffusion pathway is relevant. The question arises as to whether an extended full relaxation-matrix analysis will be capable of explaining these effects.

An important trNOE for the analysis of the orientation of the neuraminic acid side chain is the trNOE between $H7^N$ and NAc^N. This effect is also a direct trNOE, as seen from a comparison of Figs. 7b and d (cross peak 14). The spectra show several other long-range interactions for NAc^N that originate from spin diffusion (Fig. 7).

TABLE 2
INTERGLYCOSIDIC trNOEs AND SPIN-DIFFUSION EFFECTS THAT ARE OBSERVED FOR THE SIALYL LEWIS^x BOUND TO E-SELECTIN

$H1^F$	$H1^{GN}$	Spin diffusion
	$H3^{GN}$	trNOE
	$H5^{GN}$	Spin diffusion
	NAc^{GN}	trNOE
$H5^F$	$H2^G$	trNOE
	$H5^G$	Spin diffusion
	$H6^G$	trNOE and spin diffusion
	$H3^{GN}$	Spin diffusion
	$H5^{GN}$	Spin diffusion
$CH_3\text{-}6^F$	$H2^G$	trNOE
	$H5^G$	Spin diffusion
	$H6^G$	Spin diffusion
	$H3^{GN}$	Spin diffusion
$H1^G$	$H4^{GN}$	trNOE
	$H6^{GN}_{proS}$	trNOE*
	$H6^{GN}_{proR}$	trNOE*
$H3^G$	$H8^N$	trNOE
NAc^{GN}	$H2^F$	Spin diffusion
	$H5^{G,GN}$	Spin diffusion
NAc^N	$H7^N$	trNOE

New interglycosidic trNOEs are marked with an asterisk.

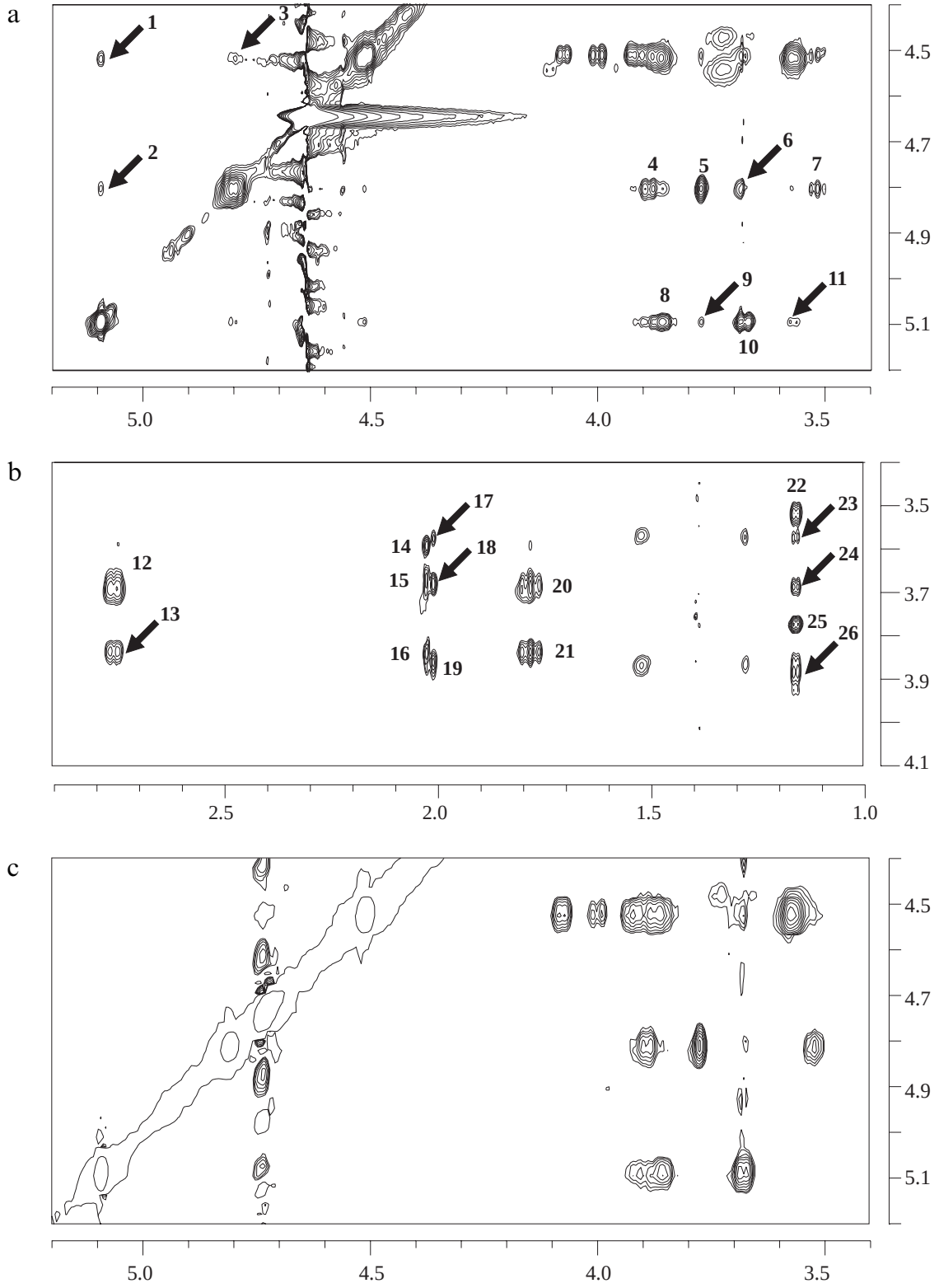

Fig. 7. Portions of a 2D trNOESY spectrum (Figs. 7a and c) and a 2D trROESY spectrum (Figs. 7b and d) are shown (600 MHz). The mixing times were 150 ms for both spectra. A comparison of the partial spectra allows one to identify spin-diffusion effects. Cross peaks discussed in the text are labeled, and cross peaks that are due to spin diffusion are identified by an additional arrow. The assignment is as follows: 1 – $H1^{F}/H1^{GN}$, 2 – $H1^{F}/H5^{F}$, 3 – $H5^{F}/H1^{G,GN}$, 4 – $H5^{F}/H3^{F}$, 5 – $H5^{F}/H4^{F}$, 6 – $H5^{F}/H6^{G}$, 7 – $H5^{F}/H2^{G}$, 8 – $H1^{F}/H3^{GN}$, 9 – $H1^{F}/H4^{F}$, 10 – $H1^{F}/H2^{F}$, 11 – $H1^{F}/H5^{GN}$, 12 – $H4^{N}/H3_{eq}{}^{N}$, 13 – $H5^{N}/H3_{eq}{}^{N}$, 14 – $H7^{N}/NAc^{N}$, 15 – $H4^{N}/NAc^{N}$, 16 – $H5^{N}/NAc^{N}$, 17 – $H5^{G,GN}/NAc^{GN}$, 18 – $H2^{F}/NAc^{GN}$, 19 – $H2^{GN}/NAc^{GN}$, 20 – $H4^{N}/H3_{ax}{}^{N}$, 21 – $H5^{N}/H3_{ax}{}^{N}$, 22 – $H2^{G}/CH_{3}$–6^{F}, 23 – $H5^{G}/CH_{3}$–6^{F}, 24 – $H6^{G}/CH_{3}$-6^{F}, 25 – $H4^{F}/CH_{3}$-6^{F}, 26 – $H3^{GN}$+$H3^{F}/CH_{3}$-6^{F}, 27 – $H3^{G}/H3_{ax}{}^{N}$. Cross peak 27 is due to an ROE of not-bound sialyl Lewis^{x} tetrasaccharide, and is not present in the 2D trNOESY spectrum because NOEs of not-bound are very close to zero at 310 K.

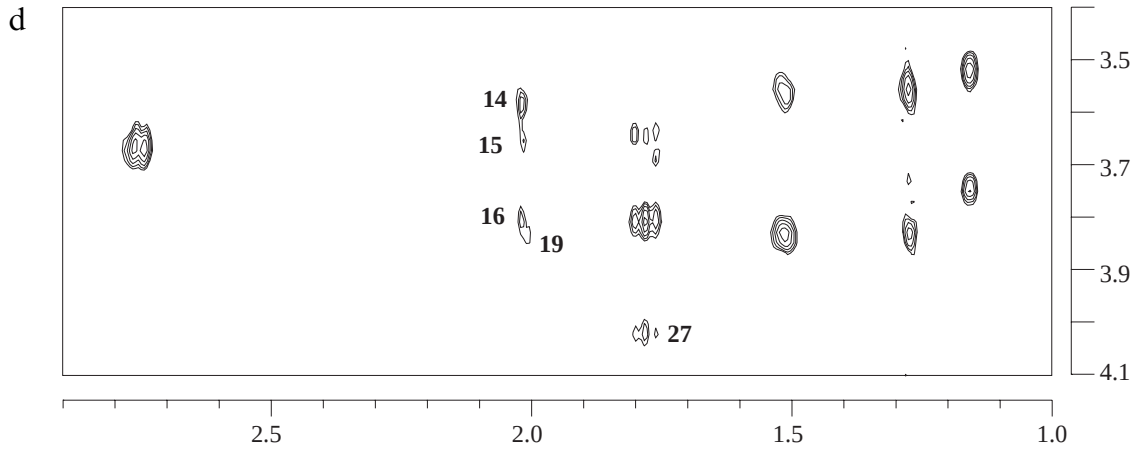

Fig. 7. (continued).

Conclusions

The NMR data presented allow an unambiguous assignment of all trNOEs and spin-diffusion effects of sialyl Lewis^x bound to E-selectin. Assignments that were reached previously on the basis of chemical shift values and steric arguments were examined, and missing assignments were completed. A concise survey of trNOEs and spin-diffusion effects that are observed for sialyl Lewis^x bound to E-selectin is presented in Table 2.

The interglycosidic trNOE between $H8^N$ and $H3^G$ (Fig. 3c) is substantial for the conformational analysis of the α-D-NeuNAc-(2→3)-β-D-Gal glycosidic linkage, and therefore it is important to assign this trNOE independently from steric arguments that were used before to exclude other possible assignments. The 3D TOCSY-trNOESY spectrum and a 1D trNOESY-TOCSY spectrum (Figs. 2 and 3) unequivocally confirm the old assignment, and the observation of a positive cross peak between $H3^G$ and $H8^N$ in a 2D trROESY spectrum makes spin-diffusion effects unlikely. Therefore, the trNOE between $H3^G$ and $H8^N$ is an important interglycosidic distance constraint that in conjunction with the absence of interglycosidic trNOEs between $H3^G$ and either $H3^N_{ax}$ or $H3^N_{eq}$ defines the bioactive conformation of the glycosidic linkage between NeuNAc and Gal.

The quantitative conformational analysis of the β-(1→4)-glycosidic linkage between Gal and GlcNAc is not possible from 2D trNOESY spectra, because the anomeric protons $H1^G$ and $H1^{GN}$ have identical chemical shift values. It is shown here that the use of a 1D TOCSY-trNOESY experiment allows one to observe trNOEs exclusively originating from $H1^G$ (Fig. 5). Two new interglycosidic trNOEs could be identified in this manner (see Table 2). The 1D TOCSY-trNOESY experiment also allows one to obtain full trNOE curves for an extended conformational analysis of the sialyl Lewis^x/E-selectin complex, which is currently in progress in our laboratory.

To summarize, our study shows that the combined use of a homonuclear 3D TOCSY-trNOESY experiment and 1D analogs of 3D NMR experiments leads to a complete and unambiguous assignment of trNOEs and spin-diffusion effects of the sialyl Lewis^x tetrasaccharide bound to E-selectin. The results obtained in this study provide a firm experimental basis for current attempts to infer the orientation of sialyl Lewis^x in the binding site of E-selectin from an extended full relaxation-matrix analysis of trNOE curves and spin-diffusion effects.

Acknowledgements

This work was supported by a grant of the Deutsche Forschungsgemeinschaft and by the Fonds der Chemischen Industrie. T.P. and J.-R.B. wish to thank NATO for a travel grant (CRG 890356). We are indebted to Prof. Dr. H. Rüterjans (Institute for Biophysical Chemistry, University of Frankfurt, Frankfurt, Germany) for giving us access to the 600 MHz spectrometer in his laboratory.

References

Arepalli, S.R., Glaudemans, C.P.J., Daves, G.D., Kovac, P. and Bax, A. (1995) *J. Magn. Reson.*, **106**, 195–198.

Asensio, J.L., Cañada, F.J. and Jimenez-Barbero, J. (1995) *Eur. J. Biochem.*, **233**, 618–630.

Bax, A. and Davis, D.G. (1985) *J. Magn. Reson.*, **65**, 355–360.

Bax, A. (1988) *J. Magn. Reson.*, **77**, 134–147.

Breg, J., Kroon-Batenburg, L.M.J., Strecker, G., Montreuil, J. and Vliegenthart, J.F.G. (1989) *Eur. J. Biochem.*, **178**, 727–739.

Cooke, R.M., Hale, R.S., Lister, S.G., Shah, G. and Malcom, P.W. (1994) *Biochemistry*, **33**, 10591–10596.

De Beer, T., Van Zuylen, C.W.E.M., Leeflang, B.R., Hard, K., Boelens, R., Kaptein, R., Kamerling, J.P. and Vliegenthart, J.F.G. (1996) *Eur. J. Biochem.*, **241**, 229–242.

De Waard, P., Leeflang, B.R., Vliegenthart, J.F.G., Boelens, R., Vuister, G.W. and Kaptein, R. (1992) *J. Biomol. NMR*, **2**, 211–226.

Emsley, L. and Bodenhausen, G. (1989) *J. Magn. Reson.*, **82**, 211–221.

Feizi, T. (1993) *Curr. Opin. Struct. Biol.*, **3**, 701–710.

Graves, B.J., Crowther, R.L., Chandran, C., Rumberger, J.M., Li, S., Huang, K.-S., Presky, D.H., Familetti, P.C., Wolitzky, B.A. and Burns, D.K. (1994) *Nature*, **367**, 532–538.

Griesinger, C., Sørensen, O.W. and Ernst, R.R. (1989) *J. Magn. Reson.*, **84**, 14–63.

Homans, S.W. and Forster, M. (1992) *Glycobiology*, **2**, 143–151.

Ichikawa, Y., Lin, Y.C., Dumas, D.P., Shen, G.-J., Garcia-Junceda, E., Williams, M.A., Bayer, R., Ketcham, C., Walker, L.E., Paulson, J.C. and Wong, C.-H. (1992) *J. Am. Chem. Soc.*, **114**, 9283–9289.

Kessler, H., Oschkinat, H. and Griesinger, C. (1986) *J. Magn. Reson.*, **70**, 106–133.

Kessler, H., Mronga, S. and Gemmecker, G. (1991) *Magn. Reson. Chem.*, **29**, 527–557.

Lasky, L.A. (1995) *Annu. Rev. Biochem.*, **64**, 113–139.

Lian, L.Y., Barsukov, I.L., Sutcliffe, M.J., Sze, K.H. and Roberts, G.C.K. (1994) *Methods Enzymol.*, **239**, 657–700.

Lin, Y.C., Hummel, C.W., Huang, D.H., Ichikawa, Y., Nicolaou, K.C. and Wong, C.H. (1992) *J. Am. Chem. Soc.*, **114**, 5452–5454.

Marion, D. and Wüthrich, K. (1983) *Biochem. Biophys. Res. Commun.*, **113**, 967–974.

Miller, K.E., Mukhapadhyay, C., Cagas, P. and Bush, C.A. (1992) *Biochemistry*, **31**, 6703–6709.

Moseley, H.N.B., Curto, E.V. and Krishna, N.R. (1995) *J. Magn. Reson.*, **B108**, 243–261.

Ni, F. and Zhu, Y. (1994) *J. Magn. Reson.*, **B102**, 180–184.

Oschkinat, H., Cieslar, C. and Griesinger, C. (1990) *J. Magn. Reson.*, **86**, 453–469.

Oschkinat, H., Müller, T. and Dieckmann, T. (1994) *Angew. Chem., Int. Ed. Engl.*, **33**, 277–293.

Peters, T., Meyer, B., Stuike-Prill, R., Somorjai, R. and Brisson, J.-R. (1993) *Carbohydr. Res.*, **238**, 49–73.

Rosen, S.D. and Bertozzi, C.R. (1994) *Curr. Opin. Cell Biol.*, **6**, 663–673.

Rutherford, T.J., Spackman, D.G., Simpson, P.J. and Homans, S.W. (1994) *Glycobiology*, **4**, 59–68.

Scheffler, K., Ernst, B., Katopodis, A., Magnani, J.L., Wang, W.T., Weisemann, R. and Peters, T. (1995) *Angew. Chem., Int. Ed. Engl.*, **34**, 1841–1844.

Scherf, T. and Anglister, J. (1993) *Biophys. J.*, **64**, 754–761.

Springer, T.A. (1995) *Annu. Rev. Physiol.*, **57**, 827–872.

Stuike-Prill, R. and Meyer, B. (1990) *Eur. J. Biochem.*, **194**, 903–919.

Subramanian, S. and Bax, A. (1987) *J. Magn. Reson.*, **71**, 325–337.

Tedder, T.F., Steeber, D.A., Douglas, A., Chen, A. and Engel, P. (1995) *FASEB J.*, **9**, 866–873.

Uhrín, D., Brisson, J.-R. and Bundle, D.R. (1993) *J. Biomol. NMR*, **3**, 367–373.

Uhrín, D., Brisson, J.-R., Kogan, G. and Jennings, H.J. (1994) *J. Magn. Reson.*, **B104**, 289–293.

Varki, A. (1994) *Proc. Natl. Acad. Sci. USA*, **91**, 7390–7397.

Vuister, G.W., De Waard, P., Boelens, R., Vliegenthart, J.F.G. and Kaptein, R. (1989) *J. Am. Chem. Soc.*, **111**, 772–774.

Weimar, T., Harris, S.L., Pitner, J.B., Bock, K. and Pinto, B.M. (1995) *Biochemistry*, **34**, 13672–13680.

Wormald, M.R., Edge, C.J. and Dwek, R.A. (1991) *Biochem. Biophys. Res. Commun.*, **180**, 1214–1221.